



New prognostic biomarker *CMTM3* in low grade glioma and its immune infiltration

Shoubin Li¹, Peng Gao¹, Xingliang Dai¹, Lei Ye¹, Zhongyong Wang², Hongwei Cheng¹

¹Department of Neurosurgery, the First Affiliated Hospital of Anhui Medical University, Hefei, China; ²Department of Neurosurgery, the Second Affiliated Hospital of Soochow University, Suzhou, China

Contributions: (I) Conception and design: H Cheng, Z Wang; (II) Administrative support: H Cheng, Z Wang; (III) Provision of study materials or patients: S Li, P Gao, X Dai; (IV) Collection and assembly of data: S Li, L Ye; (V) Data analysis and interpretation: S Li, L Ye; (VI) Manuscript writing: All authors; (VII) Final approval of manuscript: All authors.

Correspondence to: Zhongyong Wang. Department of Neurosurgery, the Second Affiliated Hospital of Soochow University, 1055 Sanxaing Road, Suzhou 215004, China. Email: wangzhongyong@suda.edu.cn; Hongwei Cheng. Department of Neurosurgery, the First Affiliated Hospital of Anhui Medical University, 218 Jixi Road, Hefei 230022, China. Email: hongwei.cheng@ahmu.edu.cn.

Background: The CKLF-like MARVEL transmembrane domain-containing 3 (*CMTM3*) is differentially expressed in a variety of tumors and closely related to tumor occurrence and progression. The expression of *CMTM3* was significantly elevated in glioma compared with normal brain tissue, to explore the potential function of *CMTM3* in the prognosis and immune infiltration of glioma has certain clinical significance.

Methods: The tumor data in this study were derived from the sequencing data of various tumors in The Cancer Genome Atlas (TCGA) database. Low-grade glioma (LGG) data in the TCGA database include sequencing and clinical data. Clinical data mainly include survival time, survival outcome, age, WHO classification and other information. Sequencing data for normal tissues were obtained from the Genotype Tissue Expression (GTEx) database. Statistical analyses were mainly performed using bioinformatics tools and the corresponding R software (version 3.6.3). The Mann-Whitney U test (Wilcoxon rank sum test) was used to compare the expression differences between the tumor group and the normal group. Survival analysis was conducted using log-rank test to compare whether the overall survival (OS) time was statistically different between the *CMTM3* high and low expression groups. The Tumor Immunity Estimation Resource (TIMER) database was used for immune infiltration analysis.

Results: The results showed that the expression of *CMTM3* in World Health Organization (WHO) II and WHO III gliomas was significantly higher than that of normal tissues ($P < 0.05$). Glioma with high *CMTM3* expression showed a lower overall survival (OS) ($P < 0.05$). Gene enrichment analysis showed that *CMTM3* was significantly enriched in 4 pathways ($FDR < 0.25$, $P < 0.05$). A high correlation was detected between *CMTM3* and a variety of immune cells. *CMTM3* is highly correlated with macrophages ($r = 0.536$, $P = 1.31 \times 10^{-36}$), dendritic cells ($r = 0.546$, $P = 2.85 \times 10^{-38}$), CD4+ T cells ($r = 0.517$, $P = 6.17 \times 10^{-34}$).

Conclusions: The *CMTM3* gene can be used as a potential prognostic marker for WHO grade II and WHO grade III glioma, is related to the immune infiltration in glioma microenvironment, and may become a new immunotherapy target.

Keywords: CKLF-like MARVEL transmembrane domain-containing 3 (*CMTM3*); bioinformatics; The Cancer Genome Atlas (TCGA); glioma

Submitted Dec 15, 2021. Accepted for publication Feb 18, 2022.

doi: 10.21037/atm-22-526

View this article at: <https://dx.doi.org/10.21037/atm-22-526>

Introduction

The revision of the World Health Organization (WHO) classification of central nervous system tumors has led to major changes in the routine diagnosis and treatment of patients with glioma (1). However, glioma remains a malignant tumor of the central nervous system with high recurrence rate, high fatality rate, and poor prognosis (2). The prognosis of different types and grades of glioma varies greatly. Although a variety of comprehensive treatment methods are used in combination, such as surgery, radiotherapy, chemotherapy, immunotherapy, electric field therapy, and neutron therapy, the treatment effect of glioma is still unsatisfactory. Therefore, it is necessary to find new treatments. CKLF-like MARVEL transmembrane domain-containing 3 (*CMTM3*) has a high correlation with immune cells, and it can be used as a potential immunotherapy target. There are many studies on prognostic markers of glioma, but there are few biomarkers recognized and widely used in the clinic. Most prognostic markers can only be used as prognostic markers alone, and their correlation with immune cells is also low, making it difficult to serve as potential therapeutic targets. As a new prognostic marker, *CMTM3* can not only judge the prognosis, but also is expected to become a potential immune target. It has a high clinical application prospect.

The expression and function of *CMTM3* in different tumor types are quite different. It shows tumor suppressor effect in some tumors while showing oncogene characteristics in other tumors. Some studies have suggested that *CMTM3* inhibits tumor cell invasion and migration in gastric cancer, liver cancer, prostate cancer, and testicular cancer, and plays the role of tumor suppressor genes (3-6). However, some others studies have shown that *CMTM3* overexpression predicts poor survival and promotes proliferation and migration of pancreatic cancer (7). Yang *et al.* (8) predicted the potential of *CMTM3* as a candidate marker for glioblastoma. Delic *et al.* (9) predicted the potential of *CMTM3* to promote tumor cell invasion by analyzing the correlation between the CMTM family and the pathogenesis of glioblastoma. However, the correlation between *CMTM3* and low-grade glioma (WHO grade II and III) and its immune infiltration are still unclear.

In this study, we used The Cancer Genome Atlas (TCGA) data to analyze the expression difference of *CMTM3* in WHO grade II and WHO grade III glioma compared to normal tissues. We analyzed the relationship between *CMTM3* and clinicopathological factors. Gene

set enrichment analysis (GSEA) was used to explore related biological processes and pathways regulated by *CMTM3*. The Tumor Immune Estimation Resource (TIMER) database was used to analyze the correlation between *CMTM3* and immune infiltration. The primary aim of this study was to demonstrate the prognostic role of *CMTM3* as a new prognostic biomarker for improving survival predictions for WHO grade II-III glioma patients. We present the following article in accordance with the REMARK reporting checklist (available at <https://atm.amegroups.com/article/view/10.21037/atm-22-526/rc>).

Methods

Data acquisition

The RNA-seq data for glioma was obtained from TCGA database (<https://portal.gdc.cancer.gov/>). The downloaded data was all WHO II and WHO III glioma data, without glioblastoma data. The RNA-seq data for normal samples was from the Genotype Tissue Expression (GTEx) database. The data of patients with significant missing information were excluded. We used two sets of data to analyze the difference in the expression of *CMTM3* in glioma and normal tissues. This study complied with the publication guidelines set by TCGA. Ethical approval and informed consent of patients were not required. The study was conducted in accordance with the Declaration of Helsinki (as revised in 2013).

Analysis of TIMER database

The TIMER (<http://cistrome.dfci.harvard.edu/TIMER/>) is a comprehensive database (10) which can be used to systematically analyze the immune infiltration of different types of cancer. The current version of TIMER contains 10,009 samples from 23 cancer types from the TCGA data set to estimate the abundance of immune infiltration. We used the TIMER online database to analyze the association of *CMTM3* with immune infiltration.

Analysis of gene set enrichment

GSEA is a computational method used to determine whether a set of a priori defined genes show statistically significant differences between 2 biological states (11). The GSEA revealed a significantly enriched gene set [false discovery rate (FDR) <0.25, P value <0.05] in *CMTM3*.

GSEA analysis looked for signaling pathways that *CMTM3* may be involved in affecting the progression of LGG (WHO grade II and WHO grade III).

Gene Expression Profiling Interaction Analysis 2 (GEPIA2) database

The GEPIA2 database was developed by Peking University as a new version of the original GEPIA. It is used to analyze the RNA sequencing expression data of 9,736 tumors and 8,587 normal samples from TCGA and GTEx projects (12). It can analyze the TCGA database online. We used it to further verify that the expression difference of *CMTM3* in LGG and normal tissues was statistically significant.

Statistical analysis

Statistical analysis and visualization were performed using the corresponding R package (R version 3.6.3; <https://www.r-project.org/>). *CMTM3* in LGG (WHO grade II and WHO grade III) and GTEx did not conform to normal distribution ($P < 0.05$ for normality test), so Mann-Whitney U test was used. The Mann-Whitney U test (Wilcoxon rank sum test) was used to compare the expression differences between the tumor group and the normal group. Survival analysis was conducted using log-rank test to compare whether the overall survival (OS) time was statistically different between the *CMTM3* high and low expression groups. The survminer package was used to draw survival curves. GO and KEGG enrichment analysis of *CMTM3*-related genes. Two different immune infiltration algorithms were used in the analysis of immune infiltration, namely the single-sample (ss) GSEA immune infiltration algorithm and the immune algorithm built in the TIMER database. The two different algorithms illustrate the correlation between *CMTM3* and immune infiltration. $P < 0.05$ was considered statistically significant. Significance levels: * $P < 0.05$, ** $P < 0.01$, *** $P < 0.001$.

Results

***CMTM3* is highly expressed in WHO grade II and III gliomata**

We downloaded the RNA-seq data of all tumor samples in TCGA database and the RNA-seq data of normal tissue samples in the GTEx database, and compared the transcription level of *CMTM3* in various tumors. It was

found that *CMTM3* was highly expressed in most tumors (Figure 1A). The ggplot2 package was used to visualize the data, and the expression of *CMTM3* in glioma and normal tissues was significantly different (Figure 1B). The GEPIA2 and Gene Expression Omnibus (GEO) databases showed that *CMTM3* is highly expressed in low-grade gliomas (LGG) (Figure 1C).

Relationship between *CMTM3* expression and clinical features of glioma

The clinical information of WHO grade II and III glioma was downloaded from TCGA database (Table 1). We compared whether there are significant differences in the expression of *CMTM3* in different clinical features between WHO grade II and III glioma. The results showed that the expression of *CMTM3* in grade II and III glioma was significantly different, and as the grade of glioma increased, the expression of *CMTM3* also increased (Figure 2A). The isocitrate dehydrogenase (IDH) in WHO grade II and III glioma was divided into wild type (WT) and mutant type (MT). The difference in *CMTM3* expression between the two groups was statistically significant (Figure 2B). The expression of *CMTM3* in the 1p/19q co-deletion group was overall lower than that of the no co-deletion group (Figure 2C). The expression level of *CMTM3* in the group older than 40 years was higher than that in the group younger than 40 years (Figure 2D).

***CMTM3* expression on the prognosis of WHO grade II and III gliomas**

A time-dependent receiver operating characteristic (ROC) curve showed that the area under the curve (AUC) of *CMTM3* predicting the 1- and 3-year survival outcomes of WHO grade II and III glioma patients were 0.821 and 0.750, indicating that *CMTM3* can predict patient survival well (Figure 3A). Kaplan-Meier survival analysis showed that *CMTM3* expression was correlated with OS in WHO grade II and III glioma patients (Figure 3B). High *CMTM3* expression indicated a poor prognosis and a lower survival rate. The survival of *CMTM3* in different clinical subgroups also had significant differences. Patients with WHO grade III gliomas with high *CMTM3* expression had lower OS and less favorable prognosis. However, WHO grade III gliomas with low *CMTM3* expression had a more favorable prognosis (Figure 3C). Additionally, *CMTM3* was highly expressed in IDH wild-type gliomas, and the OS rate was

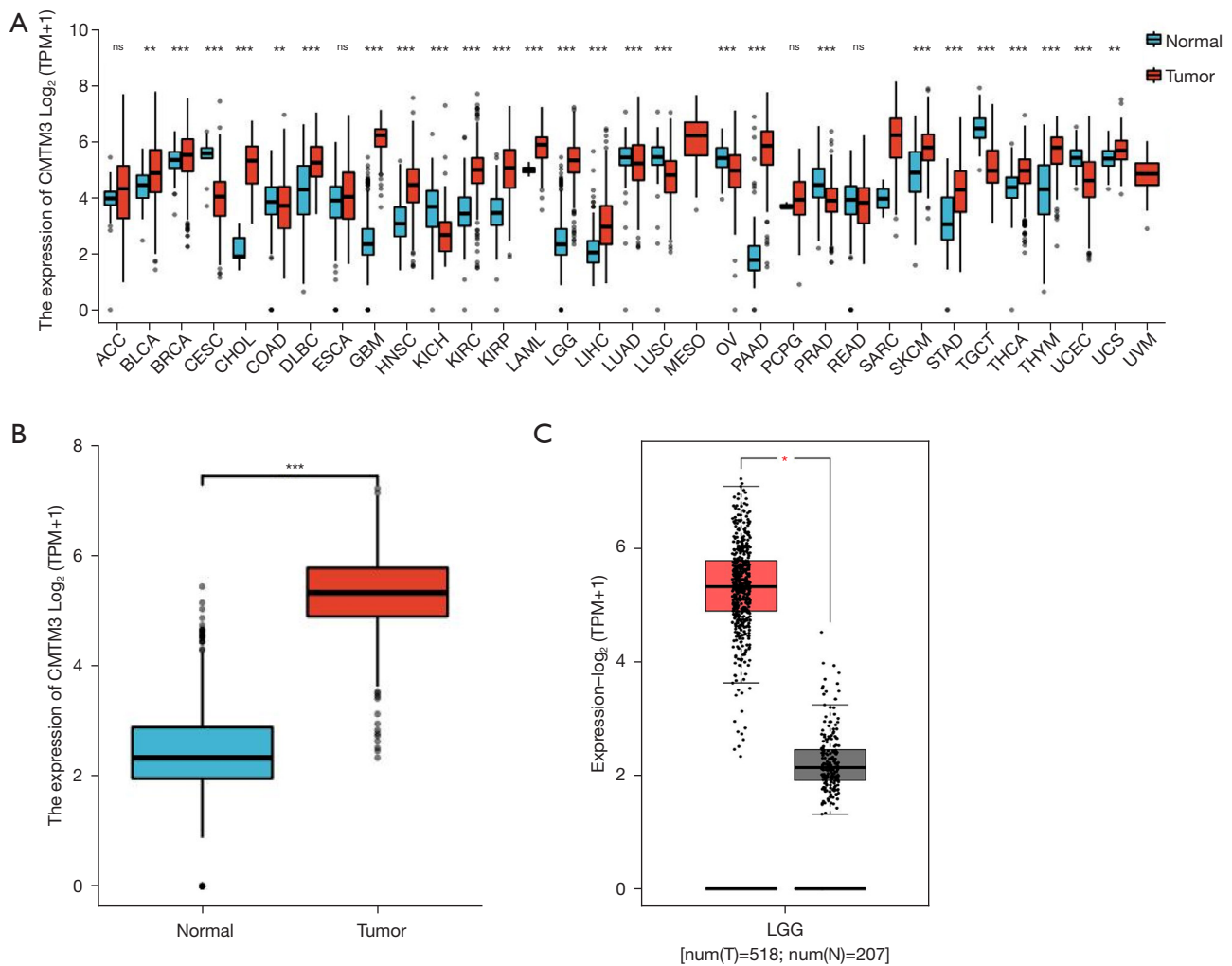


Figure 1 *CMTM3* mRNA expression levels. (A) *CMTM3* mRNA expression levels in different tumor types from TCGA database; ns, $P \geq 0.05$; (B) *CMTM3* expression levels in glioma and matched normal tissues; (C) GEPIA database shows differences in the expression of *CMTM3* in low grade glioma and normal tissues. *, $P < 0.05$; **, $P < 0.01$; ***, $P < 0.001$; ns, $P > 0.05$. ACC, adrenocortical carcinoma; BLCA, bladder urothelial carcinoma; BRCA, breast invasive carcinoma; CESC, cervical squamous cell carcinoma and endocervical adenocarcinoma; CHOL, cholangiocarcinoma; COAD, colon adenocarcinoma; DLBC, lymphoid neoplasm diffuse large B-cell lymphoma; ESCA, esophageal carcinoma; GBM, glioblastoma multiforme; HNSC, head and neck squamous cell carcinoma; KICH, kidney chromophobe; KIRC, kidney renal clear cell carcinoma; KIRP, kidney renal papillary cell carcinoma; LAML, acute myeloid leukemia; LGG, low grade glioma; LIHC, liver hepatocellular carcinoma; LUAD, lung adenocarcinoma; LUSC, lung squamous cell carcinoma; MESO, mesothelioma; OV, ovarian serous cystadenocarcinoma; PAAD, pancreatic adenocarcinoma; PCPG, pheochromocytoma and paraganglioma; PRAD, prostate adenocarcinoma; READ, rectum adenocarcinoma; SARC, sarcoma; SKCM, skin cutaneous melanoma; STAD, stomach adenocarcinoma; TGCT, testicular germ cell tumors; THCA, thyroid carcinoma; THYM, thymoma; UCEC, uterine corpus endometrial carcinoma; UCS, uterine carcinosarcoma; UVM, uveal melanoma; *CMTM3*, CKLF-like MARVEL transmembrane domain-containing 3; mRNA, messenger RNA; TCGA, The Cancer Genome Atlas; GEPIA, gene expression profiling analysis.

lower (Figure 3D). The OS rate of *CMTM3* high expression in the 1p/19q non-codeletion glioma subgroup was lower than that of the low expression group (Figure 3E). In the

subgroup of WHO grade II and III glioma patients older than 40 years, the OS curve showed that the prognosis difference between the two groups with high and low *CMTM3* expression

Table 1 Clinical related data of glioma

| Characteristic | Low expression of CMTM3 (N=264) | High expression of CMTM3 (N=264) | P value |
|--------------------------|---------------------------------|----------------------------------|---------|
| WHO grade, n (%) | | | <0.001 |
| G2 | 135 (28.9) | 89 (19.1) | |
| G3 | 95 (20.3) | 148 (31.7) | |
| IDH status, n (%) | | | <0.001 |
| WT | 17 (3.2) | 80 (15.2) | |
| Mut | 244 (46.5) | 184 (35.0) | |
| 1p/19q codeletion, n (%) | | | 0.016 |
| Codel | 99 (18.8) | 72 (13.6) | |
| Non-codel | 165 (31.2) | 192 (36.4) | |

IDH, isocitrate dehydrogenase; CMTM3, CKLF-like MARVEL transmembrane domain-containing 3; WT, wild-type; Mut, mutant; WHO, World Health Organization; codel, codeletion.

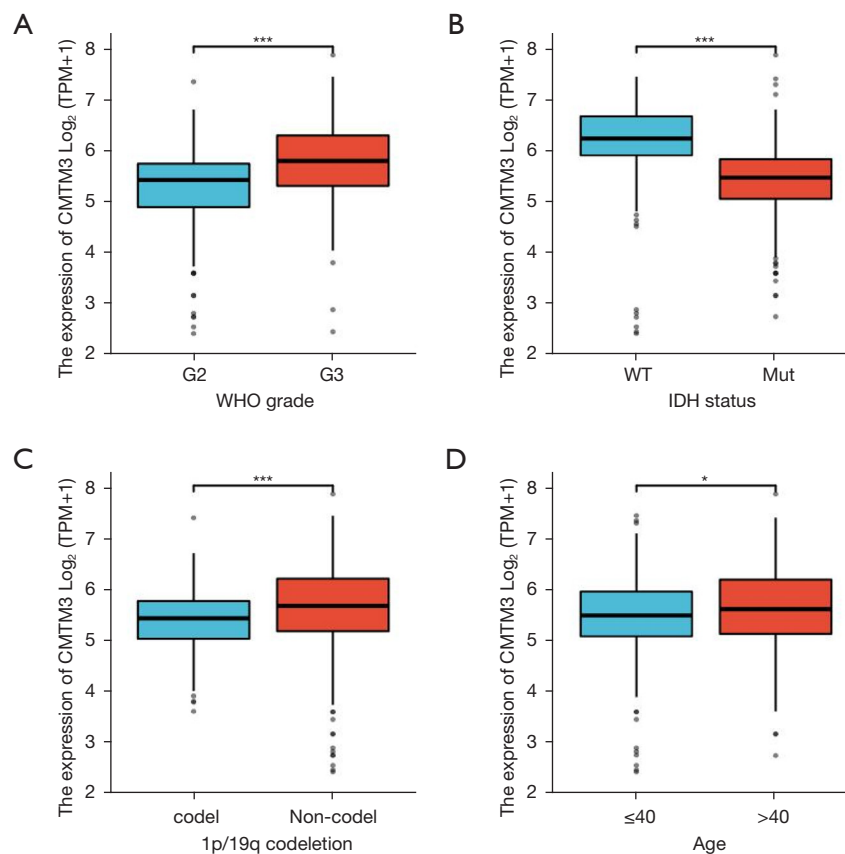


Figure 2 *CMTM3* expression and clinical features in glioma. (A) WHO grade; (B) IDH status; (C) 1p/19qcodeletion; (D) age. *, $P < 0.05$; ***, $P < 0.001$. *CMTM3*, CKLF-like MARVEL transmembrane domain-containing 3; WHO, World Health Organization.

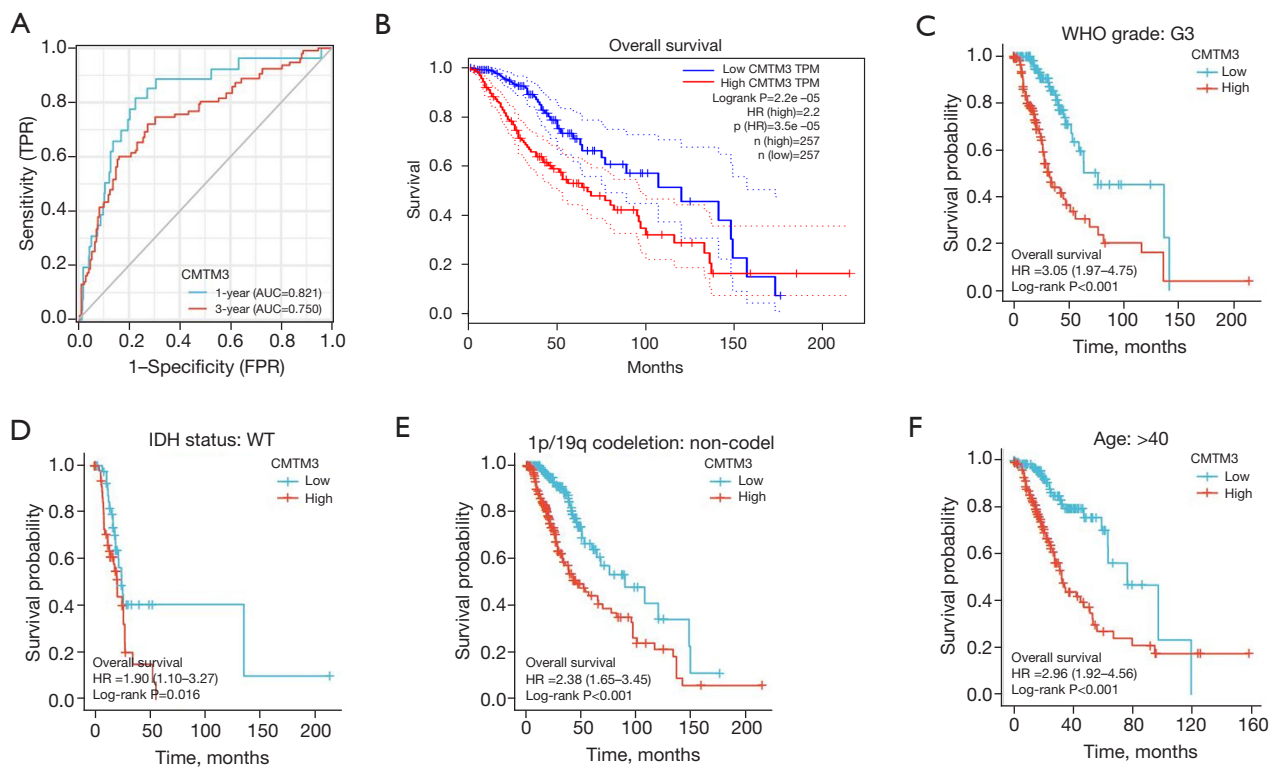


Figure 3 Prognostic analysis of *CMTM3*. (A) Time ROC curves; (B) overall survival curve of differential *CMTM3* expression in WHO grade II and III glioma; (C) OS curve of WHO grade III glioma subgroup; (D) OS curve of IDH wild-type glioma; (E) OS curve of 1p/19q non-codeletion glioma subgroup; (F) OS curve of glioma subgroup over 40 years old. *CMTM3*, CKLF-like MARVEL transmembrane domain-containing 3; OS, overall survival; IDH, isocitrate dehydrogenase.

was also statistically significant (Figure 3F).

GSEA enrichment analysis of *CMTM3* enriched pathway in LGG

We conducted GSEA to study the biological function of *CMTM3* in WHO grade II and III glioma. The GSEA showed 4 pathways where *CMTM3* was significantly enriched (FDR < 0.25, P value < 0.05) (Figure 4). The pathways included the microglial pathogen phagocytosis pathway, PLK1 pathway, IL2RB pathway, and P53 signal pathway.

Differential gene expression and gene association analysis of *CMTM3* in LGG

Comparative analysis of differential gene expression in *CMTM3* high expression and low expression groups of LGG showed that there were 138 genes with a difference

factor (log2FoldChange) greater than 2 and 128 genes with a difference of less than 2 (Figure 5A, Table 2). The Gene Ontology (GO) analysis and Kyoto Encyclopedia of Genes and Genomes (KEGG) analysis of the differential genes are shown Table 3. Genetic correlation analysis showed that the correlations between *CMTM3* and *CMTM7*, *BLNK*, *LCP2*, *CKLF*, *CMTM6*, *CMTM1*, *CMTM2*, *CMTM4*, *TTC7B*, *EEA1*, *SF3B3*, *KYNU*, *ZNF232*, *TM4SF20*, and *GPR68* had significant differences (Figure 5B). The *CMTM3* and the above-mentioned gene protein-protein interaction (PPI) network are shown in Figure 5C.

Immune infiltration analysis of *CMTM3* in LGG

The ssGSEA immune infiltration algorithm was used to calculate the correlation between *CMTM3* and 24 immune cells (Figure 6A). The results showed that *CMTM3* had the highest correlation with activated dendritic cells (aDC; $r=0.472$, $P<0.001$) and macrophages ($r=0.456$, $P<0.001$).

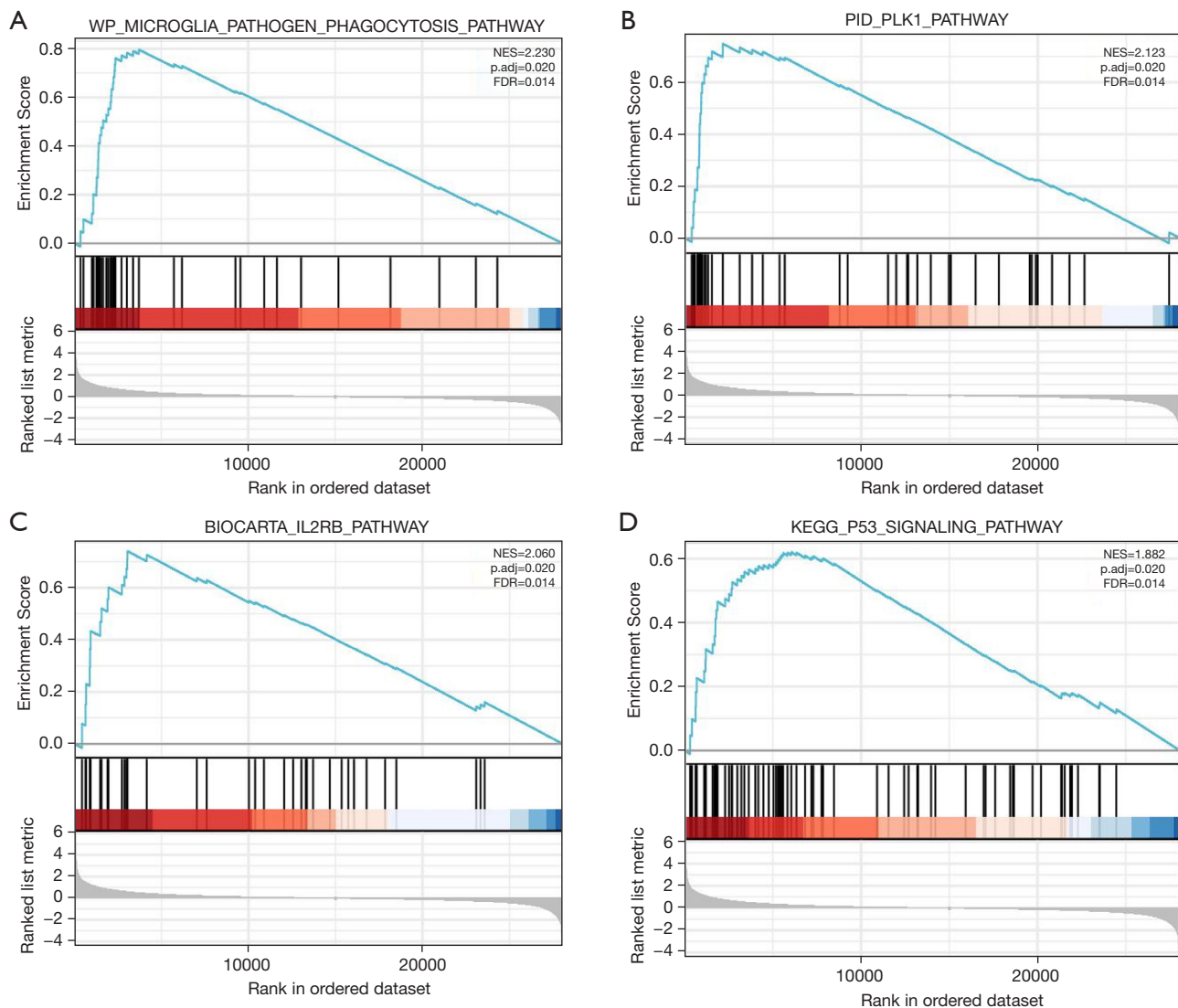


Figure 4 Enrichment plots from GSEA. (A) Microglial pathogen phagocytosis pathway; (B) PLK1 pathway; (C) IL2RB pathway; (D) P53 signal pathway. NES, normalized enrichment score; p-adj, adjusted P value; FDR, false discovery rate; GSEA, gene set enrichment analysis.

Immune checkpoints and single-gene co-expression heat maps suggested that *CMTM3* has a significant correlation with *CD274*, *PDCD1*, *CTLA4*, and *LAG3* (Figure 6B). Then, we used the TIMER tool to study the association between *CMTM3* and the level of tumor immune infiltration (Figure 6C). There were very high correlations shown for *CMTM3* and macrophages ($r=0.536$, $P=1.31e-36$), dendritic cell ($r=0.546$, $P=2.85e-38$), and $CD4^+$ T Cell ($r=0.517$, $P=6.17e-34$). The above results indicated that the expression of *CMTM3* has a high correlation with the level of immune infiltration in WHO grade II and III glioma.

Discussion

Prognostic markers can effectively evaluate and predict the clinical outcome of patients, and have been widely used in a variety of tumors, such as glioma (13), breast cancer (14), lung cancer (15), renal clear cell carcinoma (16), and others. It can reduce clinical under-treatment or over-treatment. Previous studies have found that *CMTM3* is associated with the progression of multiple diseases, and *CMTM3* has been associated with male laryngeal squamous cell carcinoma (17). Our study found that the expression of *CMTM3* was

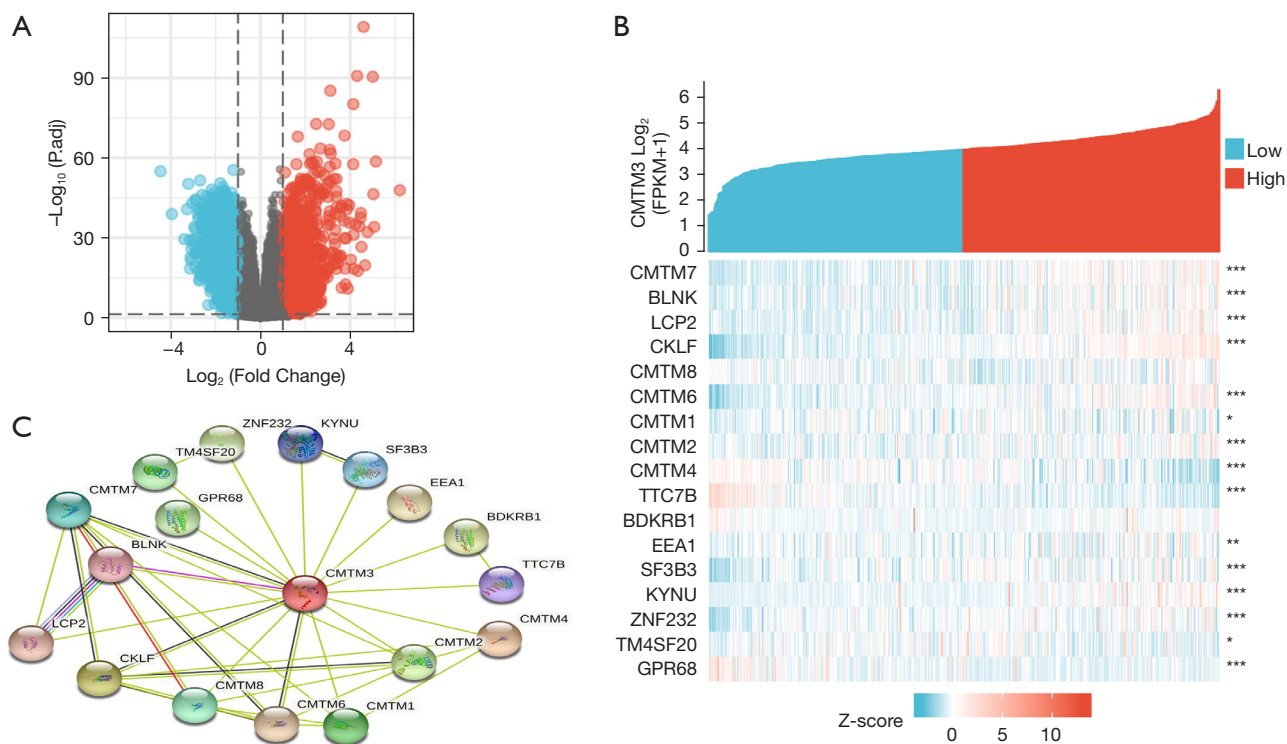


Figure 5 Gene association analysis of *CMTM3* in LGG. (A) Volcano map of differentially expressed genes in high and low expression of *CMTM3* in LGG; (B) Heat map of *CMTM3* and correlated genes; *, $P < 0.05$; **, $P < 0.01$; ***, $P < 0.001$; (C) protein interaction between *CMTM3* and related genes. LGG, low grade glioma; *CMTM3*, CKLF-like MARVEL transmembrane domain-containing 3.

Table 2 Differential gene expression of *CMTM3* high expression and low expression groups in LGG

| Gene name | $\text{log}_2\text{FoldChange}$ | Padj |
|----------------|---------------------------------|-------------|
| <i>HOXC13</i> | 5.116668651 | 1.87908E-35 |
| <i>POSTN</i> | 4.959385817 | 3.67362E-89 |
| <i>HOXB8</i> | 4.705844078 | 1.02491E-39 |
| <i>HOXB3</i> | 4.657518999 | 9.548E-114 |
| <i>HOXC11</i> | 4.652442525 | 5.00443E-31 |
| <i>C6orf15</i> | 4.644090357 | 3.09759E-20 |
| <i>HOXC9</i> | 4.597175779 | 1.12082E-41 |
| <i>HOXD13</i> | 4.513324636 | 1.45978E-36 |
| <i>PAX3</i> | 4.463324487 | 2.21132E-40 |
| <i>HOXB4</i> | 4.418414293 | 1.07868E-97 |
| <i>HOXC10</i> | 4.403236267 | 5.69058E-42 |
| <i>OTP</i> | 4.201895569 | 3.88208E-53 |
| <i>GALNT5</i> | 4.139128918 | 1.12872E-80 |
| <i>HOXD11</i> | 4.065515911 | 4.95492E-23 |
| <i>HOXD10</i> | 4.006498818 | 3.4495E-44 |

Table 2 (continued)

Table 2 (continued)

| Gene name | $\text{log}_2\text{FoldChange}$ | Padj |
|---------------|---------------------------------|-------------|
| <i>IBSP</i> | 3.798796221 | 6.08353E-45 |
| <i>VGLL2</i> | 3.789232212 | 7.14407E-40 |
| <i>HOXC8</i> | 3.782712612 | 1.64001E-30 |
| <i>PRAC2</i> | 3.728242979 | 1.68051E-26 |
| <i>HOXA6</i> | 3.713775102 | 2.59632E-18 |
| <i>HOXC6</i> | 3.660842717 | 2.36823E-44 |
| <i>HOXC12</i> | 3.606658037 | 7.77296E-12 |
| <i>TRPM8</i> | 3.5314238 | 8.05279E-68 |
| <i>ADGRG7</i> | 3.499388016 | 6.47096E-22 |
| <i>SHOX2</i> | 3.453481893 | 6.14932E-44 |
| <i>HOXA2</i> | 3.431057882 | 3.54907E-22 |
| <i>SAA1</i> | 3.396432996 | 3.61988E-33 |
| <i>HOXB5</i> | 3.343423128 | 1.31991E-40 |
| <i>IDO1</i> | 3.324235699 | 3.3799E-39 |
| <i>LBX1</i> | 3.28583822 | 6.06232E-23 |
| <i>CHI3L1</i> | 3.265815458 | 1.57582E-44 |

Table 2 (continued)

Table 2 (continued)

| Gene name | log ₂ FoldChange | Padj |
|-------------------|-----------------------------|-------------|
| <i>C7orf57</i> | 3.228683412 | 8.52261E-60 |
| <i>IGF2BP3</i> | 3.226558417 | 1.57959E-56 |
| <i>LTF</i> | 3.217130525 | 2.03887E-41 |
| <i>FAM183A</i> | 3.178076455 | 3.10142E-41 |
| <i>CA3</i> | 3.177462045 | 1.92861E-90 |
| <i>HOXB13</i> | 3.164652144 | 1.10892E-25 |
| <i>PITX2</i> | 3.160819249 | 1.73702E-39 |
| <i>HOXA4</i> | 3.149048616 | 1.14299E-21 |
| <i>SIX6</i> | 3.140442232 | 8.26446E-19 |
| <i>APCDD1L</i> | 3.095275653 | 1.60446E-37 |
| <i>MEOX2</i> | 3.07922268 | 2.60697E-40 |
| <i>AGR3</i> | 3.077692162 | 8.9839E-20 |
| <i>IGF2BP2</i> | 3.053665798 | 3.91429E-77 |
| <i>C1orf158</i> | 3.045508525 | 4.60283E-41 |
| <i>DMRTA2</i> | 3.031489903 | 5.49337E-52 |
| <i>HMGA2</i> | 3.026579035 | 2.01571E-38 |
| <i>PLEKHS1</i> | 3.018037693 | 2.56356E-45 |
| <i>NKX2-5</i> | 3.01293066 | 4.70279E-36 |
| <i>EN1</i> | 3.003903271 | 1.68623E-33 |
| <i>ABCC3</i> | 2.976055222 | 9.08704E-55 |
| <i>MMP9</i> | 2.960933955 | 2.33799E-58 |
| <i>CHRNA9</i> | 2.918733041 | 4.14357E-50 |
| <i>HOXA5</i> | 2.917582715 | 1.77877E-21 |
| <i>WT1</i> | 2.911836388 | 2.00744E-28 |
| <i>PLA2G2A</i> | 2.893234074 | 2.55948E-17 |
| <i>MAP1LC3C</i> | 2.84670752 | 4.05694E-54 |
| <i>CIBAR2</i> | 2.840278629 | 3.01785E-26 |
| <i>FOXA2</i> | 2.839959242 | 7.58558E-19 |
| <i>HOXA3</i> | 2.787675112 | 7.43244E-16 |
| <i>HOXD12</i> | 2.749005069 | 3.78518E-14 |
| <i>SRY</i> | 2.731640714 | 6.8841E-13 |
| <i>SCNN1B</i> | 2.715860729 | 1.06931E-42 |
| <i>AC013470.2</i> | 2.67828019 | 6.41459E-20 |
| <i>SPAG17</i> | 2.66851463 | 5.94338E-49 |
| <i>SAA2-SAA4</i> | 2.668349321 | 6.54478E-07 |
| <i>FOXB1</i> | 2.648331968 | 3.17655E-19 |
| <i>HOXB2</i> | 2.646456634 | 1.9897E-47 |
| <i>CXCL10</i> | 2.646342738 | 5.25735E-45 |
| <i>IGFBP2</i> | 2.645651302 | 4.46531E-62 |

Table 2 (continued)

Table 2 (continued)

| Gene name | log ₂ FoldChange | Padj |
|-----------------|-----------------------------|-------------|
| <i>MAB21L2</i> | 2.623039832 | 1.44933E-28 |
| <i>HOXA9</i> | 2.609276712 | 5.44017E-18 |
| <i>IL13RA2</i> | 2.585659092 | 4.56917E-39 |
| <i>TCTEX1D1</i> | 2.576035052 | 6.87974E-38 |
| <i>HOXA7</i> | 2.573732015 | 6.88065E-15 |
| <i>PDPN</i> | 2.572054828 | 1.39163E-57 |
| <i>FMOD</i> | 2.561917386 | 2.9601E-48 |
| <i>PRDM13</i> | 2.556914175 | 7.32592E-19 |
| <i>WDR38</i> | 2.550857828 | 1.67817E-38 |
| <i>DPEP1</i> | 2.549374003 | 3.24019E-43 |
| <i>NNMT</i> | 2.499335554 | 8.63978E-52 |
| <i>GPR139</i> | 2.493501111 | 6.81191E-17 |
| <i>GPR1</i> | 2.472611247 | 9.26844E-25 |
| <i>HP</i> | 2.427484569 | 8.13575E-32 |
| <i>H2BC9</i> | 2.403319338 | 4.74107E-27 |
| <i>ESM1</i> | 2.401817551 | 5.19493E-30 |
| <i>SPOCD1</i> | 2.391585749 | 2.70163E-41 |
| <i>ANXA1</i> | 2.346010961 | 3.83487E-57 |
| <i>SAA2</i> | 2.3343732 | 1.56859E-27 |
| <i>FAM81B</i> | 2.323524087 | 6.87369E-28 |
| <i>UNCX</i> | 2.300017197 | 3.48162E-06 |
| <i>COL3A1</i> | 2.296449403 | 6.27604E-40 |
| <i>CFAP45</i> | 2.296424396 | 5.68643E-46 |
| <i>ADAM12</i> | 2.29075902 | 1.77101E-63 |
| <i>MMP7</i> | 2.2882843 | 2.34957E-25 |
| <i>TRIM48</i> | 2.286978985 | 2.76111E-07 |
| <i>FGF3</i> | 2.284886809 | 1.25874E-05 |
| <i>CXCL9</i> | 2.278111608 | 2.49079E-37 |
| <i>OTX2</i> | 2.271472109 | 5.01914E-08 |
| <i>OSR2</i> | 2.269501718 | 2.13497E-25 |
| <i>IGLL5</i> | 2.264050095 | 3.70426E-15 |
| <i>PLAU</i> | 2.26009335 | 1.83766E-70 |
| <i>HOXA1</i> | 2.256048669 | 3.4964E-32 |
| <i>DNAH11</i> | 2.248773744 | 1.98231E-49 |
| <i>DSG2</i> | 2.243214101 | 3.75169E-23 |
| <i>PRAME</i> | 2.225962548 | 1.33066E-16 |
| <i>METTL7B</i> | 2.22189128 | 7.62525E-41 |
| <i>CER1</i> | 2.210057904 | 5.57377E-24 |
| <i>MYBPH</i> | 2.209114505 | 2.11018E-51 |

Table 2 (continued)

Table 2 (continued)

| Gene name | log ₂ FoldChange | Padj |
|-----------------|-----------------------------|-------------|
| <i>HOXA10</i> | 2.203835926 | 4.62318E-14 |
| <i>EMP3</i> | 2.200164788 | 1.50766E-45 |
| <i>C1orf189</i> | 2.1971432 | 3.71842E-36 |
| <i>TNFSF14</i> | 2.176678592 | 1.10875E-48 |
| <i>GPX8</i> | 2.164552937 | 8.62901E-51 |
| <i>C11orf88</i> | 2.155984953 | 8.57172E-32 |
| <i>TMPRSS7</i> | 2.153415552 | 3.09339E-26 |
| <i>RASEF</i> | 2.152854493 | 1.80182E-42 |
| <i>TIMP1</i> | 2.143857143 | 1.63342E-40 |
| <i>HLA-DQA2</i> | 2.141690362 | 2.74272E-26 |
| <i>HOXB9</i> | 2.114900842 | 2.14804E-13 |
| <i>CHRNA1</i> | 2.112533921 | 1.56397E-26 |
| <i>CLEC12A</i> | 2.108393213 | 7.23658E-35 |
| <i>LIF</i> | 2.107516234 | 1.9219E-39 |
| <i>HOXB7</i> | 2.106584277 | 4.71654E-38 |
| <i>GDF15</i> | 2.090663327 | 7.08461E-35 |
| <i>TEKT1</i> | 2.088363812 | 1.42056E-31 |
| <i>ARL14EPL</i> | 2.083088605 | 2.10933E-14 |
| <i>TFAP2B</i> | 2.080092571 | 2.35245E-10 |
| <i>DRC1</i> | 2.064038168 | 1.5917E-22 |
| <i>COL1A1</i> | 2.050151005 | 1.96802E-33 |
| <i>FCGBP</i> | 2.031570526 | 1.05493E-41 |
| <i>ABCB11</i> | 2.023535703 | 1.46968E-19 |
| <i>EDDM3A</i> | 2.021155161 | 3.87184E-09 |
| <i>ADGRE1</i> | 2.011136139 | 6.4663E-35 |
| <i>SIM1</i> | 2.007166223 | 1.36406E-08 |
| <i>APOL4</i> | 2.003837857 | 8.41203E-40 |
| <i>HOXD9</i> | 2.003654741 | 4.88096E-14 |
| <i>EYA4</i> | 2.000149979 | 7.62686E-27 |
| <i>KCNT1</i> | -2.000425656 | 9.49434E-45 |
| <i>SYT13</i> | -2.004447708 | 2.04222E-36 |
| <i>MTUS2</i> | -2.007046581 | 2.9601E-48 |
| <i>NEFH</i> | -2.008667688 | 3.48069E-43 |
| <i>PHF24</i> | -2.009771634 | 8.32623E-41 |
| <i>TMEM130</i> | -2.010732944 | 4.90611E-39 |
| <i>KRT3</i> | -2.011084541 | 1.81158E-16 |
| <i>GPR83</i> | -2.011221274 | 2.77435E-36 |
| <i>KCNB2</i> | -2.016021649 | 9.25369E-33 |
| <i>KRT31</i> | -2.016394462 | 2.88513E-24 |

Table 2 (continued)

Table 2 (continued)

| Gene name | log ₂ FoldChange | Padj |
|----------------|-----------------------------|-------------|
| <i>GRIN1</i> | -2.017448395 | 3.04826E-37 |
| <i>GAD2</i> | -2.017560605 | 9.71647E-32 |
| <i>SERTM1</i> | -2.029232159 | 1.91892E-29 |
| <i>PTPRR</i> | -2.044425941 | 6.25345E-44 |
| <i>CRH</i> | -2.046969921 | 1.40043E-30 |
| <i>SOHLH1</i> | -2.052409159 | 1.74515E-29 |
| <i>ATP2B3</i> | -2.056609799 | 1.76487E-43 |
| <i>TRHDE</i> | -2.058854329 | 1.44864E-34 |
| <i>GSG1L2</i> | -2.061166978 | 1.47503E-17 |
| <i>C3orf80</i> | -2.075082068 | 4.52202E-42 |
| <i>HS6ST3</i> | -2.080328765 | 5.87947E-37 |
| <i>SYNPR</i> | -2.082987743 | 3.71978E-34 |
| <i>SMPX</i> | -2.083532956 | 1.1917E-25 |
| <i>GJB6</i> | -2.083864735 | 2.89147E-23 |
| <i>TPH2</i> | -2.08951245 | 3.38212E-34 |
| <i>EIF4E1B</i> | -2.092218775 | 3.35481E-36 |
| <i>SNAP25</i> | -2.101842462 | 9.16283E-47 |
| <i>GDA</i> | -2.10403187 | 6.12622E-33 |
| <i>CHRNA2</i> | -2.104618542 | 8.22836E-30 |
| <i>SLC17A7</i> | -2.107615563 | 3.92674E-29 |
| <i>FRMPD4</i> | -2.110734929 | 1.95618E-41 |
| <i>CRYM</i> | -2.111883079 | 7.37337E-33 |
| <i>HTR1A</i> | -2.117518812 | 1.24888E-33 |
| <i>GPR52</i> | -2.119268119 | 4.98229E-23 |
| <i>SLC22A8</i> | -2.122612999 | 1.82013E-26 |
| <i>CPNE9</i> | -2.130126324 | 3.57179E-52 |
| <i>CBLN2</i> | -2.132829171 | 1.34102E-51 |
| <i>UNC13C</i> | -2.135690586 | 2.36984E-37 |
| <i>RXFP1</i> | -2.142677783 | 1.13744E-41 |
| <i>GABRA4</i> | -2.146199486 | 1.51401E-34 |
| <i>STAT4</i> | -2.149687961 | 8.04074E-47 |
| <i>PCDHGA3</i> | -2.149961068 | 9.09778E-48 |
| <i>NWD2</i> | -2.159704642 | 3.07876E-28 |
| <i>KLK5</i> | -2.169160593 | 4.79592E-24 |
| <i>CAMK1G</i> | -2.173018216 | 1.45869E-33 |
| <i>SH2D5</i> | -2.176716893 | 1.66794E-46 |
| <i>LHFPL5</i> | -2.179416319 | 6.58393E-33 |
| <i>CIDEA</i> | -2.192702209 | 8.20581E-35 |
| <i>BHLHA9</i> | -2.207783811 | 7.76714E-24 |

Table 2 (continued)

Table 2 (continued)

| Gene name | log ₂ FoldChange | Padj |
|------------------|-----------------------------|-------------|
| <i>RYR2</i> | -2.208932724 | 6.30081E-42 |
| <i>MAP7D2</i> | -2.210547901 | 5.36904E-39 |
| <i>MEPE</i> | -2.223714424 | 3.10448E-23 |
| <i>SSTR4</i> | -2.226967435 | 3.55716E-29 |
| <i>ANKRD30B</i> | -2.232170903 | 3.2962E-41 |
| <i>NEFL</i> | -2.2343183 | 1.73422E-30 |
| <i>SLC6A17</i> | -2.237086072 | 1.3379E-45 |
| <i>VIP</i> | -2.237640471 | 3.97619E-49 |
| <i>PRKCG</i> | -2.248658823 | 1.11483E-40 |
| <i>IQCF3</i> | -2.250441258 | 1.87159E-17 |
| <i>OPRM1</i> | -2.25557997 | 6.8728E-25 |
| <i>TMEM155</i> | -2.255748661 | 6.02301E-40 |
| <i>SLC12A5</i> | -2.262088143 | 8.56124E-54 |
| <i>SLC22A9</i> | -2.266565009 | 2.02681E-29 |
| <i>FAM153B</i> | -2.269323003 | 4.54784E-38 |
| <i>KRT222</i> | -2.283038129 | 4.75164E-46 |
| <i>SYT1</i> | -2.286460252 | 1.12829E-45 |
| <i>CREG2</i> | -2.299541073 | 1.23291E-39 |
| <i>NRGN</i> | -2.300300418 | 2.33789E-40 |
| <i>PNPLA5</i> | -2.30135478 | 2.37149E-32 |
| <i>SULT4A1</i> | -2.308305659 | 2.09569E-43 |
| <i>LINC02218</i> | -2.310141943 | 2.97638E-16 |
| <i>TBR1</i> | -2.31485039 | 4.4055E-42 |
| <i>LYPD8</i> | -2.321248192 | 7.35857E-34 |
| <i>KLK7</i> | -2.324326189 | 9.5428E-28 |
| <i>PVALB</i> | -2.328814713 | 1.37338E-31 |
| <i>RBFOX1</i> | -2.336287076 | 3.21666E-50 |
| <i>HIPK4</i> | -2.339576763 | 2.88514E-41 |
| <i>CCK</i> | -2.339668985 | 4.05528E-41 |
| <i>GPR22</i> | -2.341595608 | 1.85966E-43 |
| <i>PNMA6F</i> | -2.350264426 | 1.51401E-34 |
| <i>PROKR2</i> | -2.362931824 | 4.45719E-33 |
| <i>HNF4A</i> | -2.36367229 | 1.03574E-31 |
| <i>SDR16C5</i> | -2.37396754 | 2.37806E-40 |
| <i>RGS4</i> | -2.379681544 | 9.1091E-45 |
| <i>STYK1</i> | -2.385309519 | 5.7256E-42 |
| <i>C1QL3</i> | -2.404478753 | 5.47936E-34 |
| <i>C11orf87</i> | -2.405081729 | 1.50335E-42 |
| <i>DDN</i> | -2.409162361 | 7.2157E-47 |

Table 2 (continued)

Table 2 (continued)

| Gene name | log ₂ FoldChange | Padj |
|-----------------|-----------------------------|-------------|
| <i>PACSLN1</i> | -2.412698014 | 1.29868E-42 |
| <i>SSTR3</i> | -2.41316214 | 2.18925E-42 |
| <i>MPPED1</i> | -2.436543 | 5.30699E-46 |
| <i>OLFM3</i> | -2.440603613 | 4.52253E-50 |
| <i>HTR1E</i> | -2.440659107 | 7.42541E-37 |
| <i>MAL2</i> | -2.451794291 | 7.89009E-45 |
| <i>CALHM1</i> | -2.472381369 | 1.77177E-44 |
| <i>CACNG3</i> | -2.474271337 | 7.39057E-40 |
| <i>HCN1</i> | -2.476812891 | 7.14877E-46 |
| <i>KCNS2</i> | -2.504945295 | 5.50985E-43 |
| <i>SV2B</i> | -2.524182665 | 9.8185E-47 |
| <i>MAS1</i> | -2.547665168 | 1.98423E-33 |
| <i>KCNH5</i> | -2.555303851 | 4.3273E-47 |
| <i>HTR5A</i> | -2.559349382 | 4.31794E-47 |
| <i>TNNT2</i> | -2.563464962 | 2.43606E-37 |
| <i>GABRA1</i> | -2.581986894 | 7.40714E-45 |
| <i>NGB</i> | -2.591432149 | 2.30754E-40 |
| <i>VSNL1</i> | -2.596535624 | 4.75164E-46 |
| <i>THEG</i> | -2.596738717 | 6.28538E-36 |
| <i>GABRB2</i> | -2.613968264 | 2.66929E-52 |
| <i>ANKRD34C</i> | -2.630980278 | 7.98845E-48 |
| <i>CAMK2A</i> | -2.631334534 | 4.81438E-48 |
| <i>FADS6</i> | -2.647147861 | 5.12482E-45 |
| <i>NEFM</i> | -2.671792682 | 3.92308E-47 |
| <i>SLC6A7</i> | -2.710308802 | 8.56433E-43 |
| <i>GABRA6</i> | -2.712321306 | 3.60028E-39 |
| <i>KCNV1</i> | -2.71696464 | 3.365E-37 |
| <i>CNGB1</i> | -2.769480631 | 3.60028E-39 |
| <i>KCNS1</i> | -2.770816079 | 2.0511E-41 |
| <i>SOWAHB</i> | -2.824115288 | 1.26022E-58 |
| <i>ROS1</i> | -2.876421103 | 8.17676E-42 |
| <i>NEUROD6</i> | -2.922410812 | 3.14136E-43 |
| <i>GPR26</i> | -2.949633127 | 7.65748E-44 |
| <i>OR14I1</i> | -2.972889534 | 9.75109E-33 |
| <i>NPBWR2</i> | -3.042387614 | 2.16054E-28 |
| <i>MCHR2</i> | -3.108660041 | 8.14598E-40 |
| <i>HTR3B</i> | -3.172728665 | 2.33878E-48 |
| <i>TESPA1</i> | -3.352010134 | 3.06579E-56 |
| <i>CTXN3</i> | -3.55912291 | 1.86724E-50 |
| <i>CARTPT</i> | -4.422650231 | 8.85939E-55 |

CMTM3, CKLF-like MARVEL transmembrane domain-containing 3; LGG, low grade glioma.

Table 3 GO and KEGG analysis of differential gene expression in *CMTM3* high expression and low expression groups

| Ontology | ID | Description | Gene ratio | Bg ratio | P value | p.adjust | q value |
|----------|------------|--|------------|------------|----------|----------|----------|
| BP | GO:0007389 | Pattern specification process | 41/230 | 446/18,670 | 3.91e-24 | 7.26e-21 | 6.24e-21 |
| BP | GO:0009952 | Anterior/posterior pattern specification | 31/230 | 219/18,670 | 5.22e-24 | 7.26e-21 | 6.24e-21 |
| BP | GO:0003002 | Regionalization | 36/230 | 351/18,670 | 7.42e-23 | 6.88e-20 | 5.91e-20 |
| BP | GO:0048706 | Embryonic skeletal system development | 23/230 | 126/18,670 | 1.21e-20 | 8.42e-18 | 7.23e-18 |
| BP | GO:0048704 | Embryonic skeletal system morphogenesis | 19/230 | 93/18,670 | 3.19e-18 | 1.78e-15 | 1.53e-15 |
| CC | GO:0034702 | Ion channel complex | 20/244 | 301/19,717 | 1.20e-09 | 3.45e-07 | 2.76e-07 |
| CC | GO:1902495 | Transmembrane transporter complex | 20/244 | 324/19,717 | 4.27e-09 | 6.12e-07 | 4.90e-07 |
| CC | GO:1990351 | Transporter complex | 20/244 | 332/19,717 | 6.46e-09 | 6.18e-07 | 4.94e-07 |
| CC | GO:0097060 | Synaptic membrane | 22/244 | 432/19,717 | 2.35e-08 | 1.69e-06 | 1.35e-06 |
| CC | GO:0099060 | Integral component of postsynaptic Specialization membrane | 8/244 | 74/19,717 | 3.66e-06 | 1.82e-04 | 1.46e-04 |
| MF | GO:0022839 | Ion gated channel activity | 24/232 | 334/17,697 | 1.46e-11 | 3.52e-09 | 2.73e-09 |
| MF | GO:0022836 | Gated channel activity | 24/232 | 343/17,697 | 2.56e-11 | 3.52e-09 | 2.73e-09 |
| MF | GO:0001228 | DNA-binding transcription activator activity, RNA polymerase II-specific | 27/232 | 439/17,697 | 2.67e-11 | 3.52e-09 | 2.73e-09 |
| MF | GO:0005216 | Ion channel activity | 25/232 | 416/17,697 | 2.48e-10 | 2.46e-08 | 1.91e-08 |
| MF | GO:0022838 | Substrate-specific channel activity | 25/232 | 428/17,697 | 4.50e-10 | 3.56e-08 | 2.76e-08 |
| KEGG | hsa04080 | Neuroactive ligand-receptor interaction | 22/96 | 341/8,076 | 4.54e-11 | 7.95e-09 | 7.31e-09 |
| KEGG | hsa05033 | Nicotine addiction | 6/96 | 40/8,076 | 6.68e-06 | 4.29e-04 | 3.95e-04 |
| KEGG | hsa04742 | Taste transduction | 8/96 | 86/8,076 | 7.36e-06 | 4.29e-04 | 3.95e-04 |
| KEGG | hsa04727 | GABAergic synapse | 7/96 | 89/8,076 | 8.38e-05 | 0.004 | 0.003 |
| KEGG | hsa04726 | Serotonergic synapse | 7/96 | 115/8,076 | 4.15e-04 | 0.015 | 0.013 |

GO, Gene Ontology; KEGG, Kyoto Encyclopedia of Genes Genomes; *CMTM3*, CKLF-like MARVEL transmembrane domain-containing 3.

significantly increased in glioma, and patients with high *CMTM3* expression had a lower OS time. Therefore, it is reasonable to believe that the high expression of *CMTM3* will promote the progression of glioma. Subsequently, the relationship between the expression of *CMTM3* and the clinical characteristics of glioma was analyzed. The results showed that the expression of *CMTM3* in WHO grade III glioma was significantly higher than that in WHO grade II. The IDH wild-type glioma had higher expression of *CMTM3* than IDH mutant-type. The expression of *CMTM3* in patients with 1p/19q non-codeletion glioma was significantly higher than that of those with 1p/19q codeletion. Clinically, patients with WHO grade III, IDH wild-type, and 1p/19q non-codeletion often have a poor prognosis. Our study showed that the high expression of *CMTM3* was closely related to the poor prognosis of

glioma. The survival curve showed that the OS of patients with high expression of *CMTM3* glioma was significantly lower than that of those with low expression of *CMTM3*. Therefore, the prognosis of glioma patients can be predicted alternatively by detecting the expression of *CMTM3*.

Time-dependent ROC can be applied to the prediction of multiple biomarkers. It can predict the survival rate of patients. In this study, the time-dependent ROC curve was drawn to predict the 1- and 3-year survival outcomes of patients, and the AUC was 0.821 and 0.750. This shows that *CMTM3* has high predictive value and can predict the survival of patients with glioma. We used GSEA to evaluate the molecular mechanisms of prognostic genes and determine the related pathways. We also used GSEA to find 4 related pathways in LGG together with high expression of *CMTM3*. The enrichment results showed that

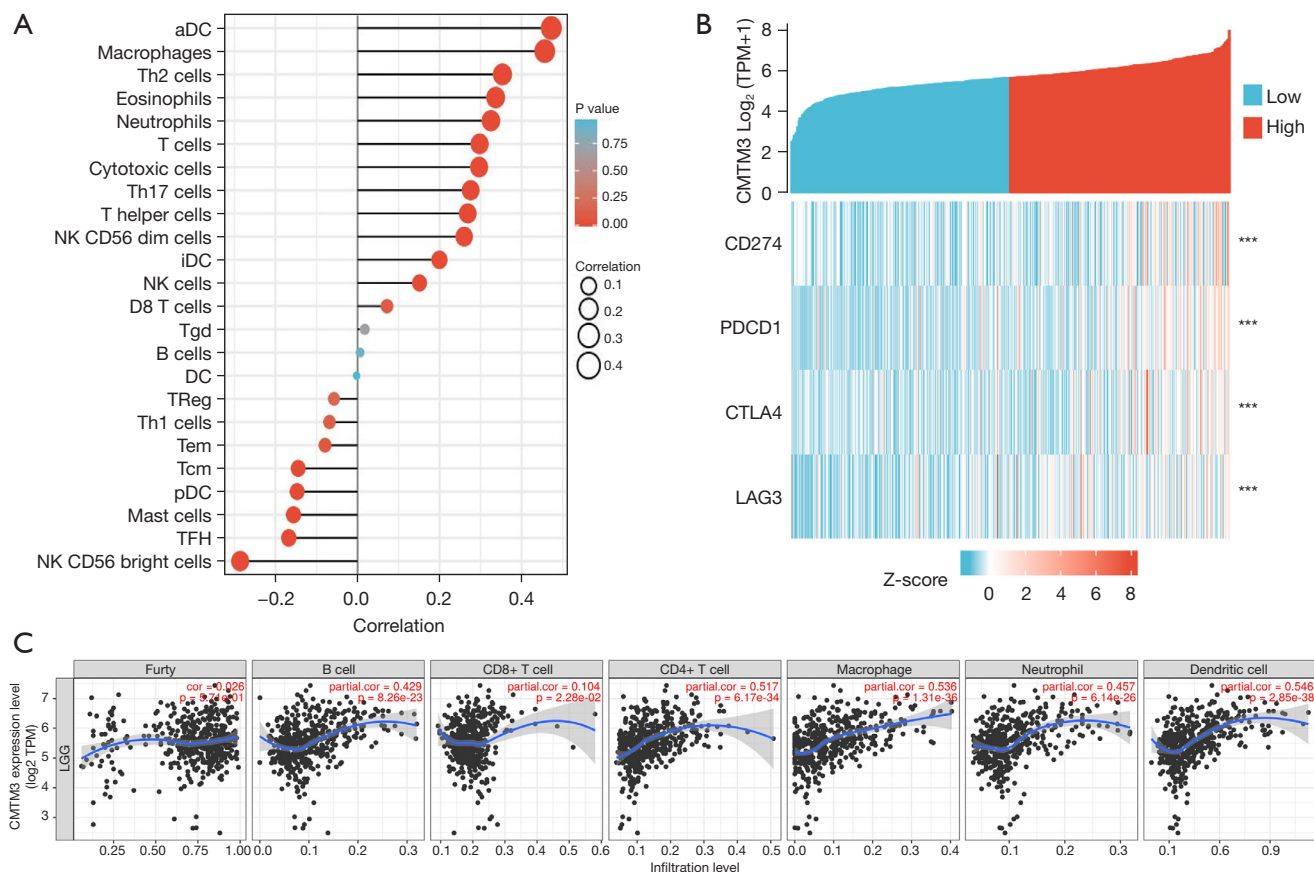


Figure 6 Correlation analysis between *CMTM3* and immune cells. (A) ssGSEA immune infiltration algorithm calculated the correlation between *CMTM3* and 24 immune cells; (B) immune checkpoints and single-gene co-expression heat maps; ***, $P < 0.001$; (C) correlations between *CMTM3* expression and immune infiltration levels in LGG by TIMER database. *CMTM3*, CKLF-like MARVEL transmembrane domain-containing 3; ssGSEA, single-sample gene set enrichment analysis; LGG, low grade glioma.

CMTM3 was significantly enriched in 4 gene sets, and may affect the progression of glioma through these pathways. These 4 pathways have been shown to be related to many diseases, such as liver fibrosis (18), glioblastoma (19), and so on. Cancer immunotherapy is an important method of treating cancer, in which the patients' own immune system is used to fight tumors (20), thus it has been widely used in the treatment of a variety of tumors (21). Cancer immunotherapy urgently needs biomarkers to accurately predict clinical response, and it has been applied to glioma (22,23). Immune infiltration analysis found that *CMTM3* is highly correlated with a variety of immune cells, such as B cell, CD8⁺ T cell, CD4⁺ T cell, macrophage, neutrophil, and dendritic cell. Together, our results indicate that *CMTM3* may be a new target for immunotherapy response in glioma. This research was based on bioinformatics and provides new ideas and research directions for follow-up research. It was not

a prospective study, so there is the possibility of confounding factors. In future, the specific mechanism of *CMTM3* on WHO II and WHO III gliomas needs to be further studied with multi-center experimental data verification.

Conclusions

Through bioinformatics analyses, we found that the expression of *CMTM3* in WHO II and WHO III gliomas was significantly higher than that in normal tissues. The *CMTM3* gene is a potential prognostic marker for WHO grade II and III gliomas, and is closely related to the immune infiltration of glioma.

Acknowledgments

Funding: This work was supported by the youth medical doctors

project of Jiangsu Province, China (No. QNRC2016870) and Project of Suzhou Health Talents, China (No. 2020090).

Footnote

Reporting Checklist: The authors have completed the REMARK reporting checklist. Available at <https://atm.amegroupp.com/article/view/10.21037/atm-22-526/rc>

Conflicts of Interest: All authors have completed the ICMJE uniform disclosure form (available at <https://atm.amegroupp.com/article/view/10.21037/atm-22-526/coif>). The authors have no conflicts of interest to declare.

Ethical Statement: The authors are accountable for all aspects of the work in ensuring that questions related to the accuracy or integrity of any part of the work are appropriately investigated and resolved. The study was conducted in accordance with the Declaration of Helsinki (as revised in 2013).

Open Access Statement: This is an Open Access article distributed in accordance with the Creative Commons Attribution-NonCommercial-NoDerivs 4.0 International License (CC BY-NC-ND 4.0), which permits the non-commercial replication and distribution of the article with the strict proviso that no changes or edits are made and the original work is properly cited (including links to both the formal publication through the relevant DOI and the license). See: <https://creativecommons.org/licenses/by-nc-nd/4.0/>.

References

1. Weller M, van den Bent M, Preusser M, et al. EANO guidelines on the diagnosis and treatment of diffuse gliomas of adulthood. *Nat Rev Clin Oncol* 2021;18:170-86.
2. Tan AC, Ashley DM, López GY, et al. Management of glioblastoma: State of the art and future directions. *CA Cancer J Clin* 2020;70:299-312.
3. Lu M, Huang Y, Sun W, et al. miR-135b-5p promotes gastric cancer progression by targeting CMTM3. *Int J Oncol* 2018;52:589-98.
4. Li W, Zhang S. CKLF-Like MARVEL Transmembrane Domain-Containing Member 3 (CMTM3) Inhibits the Proliferation and Tumorigenesis in Hepatocellular Carcinoma Cells. *Oncol Res* 2017;25:285-93.
5. Hu F, Yuan W, Wang X, et al. CMTM3 is reduced in prostate cancer and inhibits migration, invasion and growth of LNCaP cells. *Clin Transl Oncol* 2015;17:632-9.
6. Li Z, Xie J, Wu J, et al. CMTM3 inhibits human testicular cancer cell growth through inducing cell-cycle arrest and apoptosis. *PLoS One* 2014;9:e88965.
7. Zhou Z, Ma Z, Li Z, et al. CMTM3 Overexpression Predicts Poor Survival and Promotes Proliferation and Migration in Pancreatic Cancer. *J Cancer* 2021;12:5797-806.
8. Yang Q, Wang R, Wei B, et al. Candidate Biomarkers and Molecular Mechanism Investigation for Glioblastoma Multiforme Utilizing WGCNA. *Biomed Res Int* 2018;2018:4246703.
9. Delic S, Thuy A, Schulze M, et al. Systematic investigation of CMTM family genes suggests relevance to glioblastoma pathogenesis and CMTM1 and CMTM3 as priority targets. *Genes Chromosomes Cancer* 2015;54:433-43.
10. Li T, Fan J, Wang B, et al. TIMER: A Web Server for Comprehensive Analysis of Tumor-Infiltrating Immune Cells. *Cancer Res* 2017;77:e108-10.
11. Subramanian A, Kuehn H, Gould J, et al. GSEA-P: a desktop application for Gene Set Enrichment Analysis. *Bioinformatics* 2007;23:3251-3.
12. Tang Z, Kang B, Li C, et al. GEPIA2: an enhanced web server for large-scale expression profiling and interactive analysis. *Nucleic Acids Res* 2019;47:W556-60.
13. Kristensen BW, Priesterbach-Ackley LP, Petersen JK, et al. Molecular pathology of tumors of the central nervous system. *Ann Oncol* 2019;30:1265-78.
14. Cocco S, Piezzo M, Calabrese A, et al. Biomarkers in Triple-Negative Breast Cancer: State-of-the-Art and Future Perspectives. *Int J Mol Sci* 2020;21:4579.
15. Seijo LM, Peled N, Ajona D, et al. Biomarkers in Lung Cancer Screening: Achievements, Promises, and Challenges. *J Thorac Oncol* 2019;14:343-57.
16. Lin J, Yu M, Xu X, et al. Identification of biomarkers related to CD8+ T cell infiltration with gene co-expression network in clear cell renal cell carcinoma. *Aging (Albany NY)* 2020;12:3694-712.
17. Xie J, Yuan Y, Liu Z, et al. CMTM3 is frequently reduced in clear cell renal cell carcinoma and exhibits tumor suppressor activities. *Clin Transl Oncol* 2014;16:402-9.
18. Chen Y, Chen X, Ji YR, et al. PLK1 regulates hepatic stellate cell activation and liver fibrosis through Wnt/ β -catenin signalling pathway. *J Cell Mol Med* 2020;24:7405-16.
19. Lan Y, Lou J, Hu J, et al. Downregulation of SNRPG induces cell cycle arrest and sensitizes human glioblastoma cells to temozolomide by targeting Myc through a p53-dependent signaling pathway. *Cancer Biol Med*

- 2020;17:112-31.
20. Gohil SH, Iorgulescu JB, Braun DA, et al. Applying high-dimensional single-cell technologies to the analysis of cancer immunotherapy. *Nat Rev Clin Oncol* 2021;18:244-56.
 21. Meric-Bernstam F, Larkin J, Tabernero J, et al. Enhancing anti-tumour efficacy with immunotherapy combinations. *Lancet* 2021;397:1010-22.
 22. Tang B, Guo ZS, Bartlett DL, et al. Synergistic

- Combination of Oncolytic Virotherapy and Immunotherapy for Glioma. *Clin Cancer Res* 2020;26:2216-30.
23. Chen L, Qin D, Guo X, et al. Putting Proteomics Into Immunotherapy for Glioblastoma. *Front Immunol* 2021;12:593255.

(English Language Editor: J. Jones)

Cite this article as: Li S, Gao P, Dai X, Ye L, Wang Z, Cheng H. New prognostic biomarker *CMTM3* in low grade glioma and its immune infiltration. *Ann Transl Med* 2022;10(4):206. doi: 10.21037/atm-22-526